

The Lattice Free Energy with Overlap Fermions: A Two-Loop Result

A. Athenodorou and H. Panagopoulos

Department of Physics, University of Cyprus, P.O. Box 20537, Lefkosia CY-1678, Cyprus

email: ph00aa1@ucy.ac.cy, haris@ucy.ac.cy

(November 19, 2018)

Abstract

We calculate the 2-loop partition function of QCD on the lattice, using the Wilson formulation for gluons and the overlap-Dirac operator for fermions. Direct by-products of our result are the 2-loop free energy and average plaquette.

Our calculation serves also as a prototype for further higher loop calculations in the overlap formalism.

We present our results as a function of a free parameter M_0 entering the overlap action; the dependence on the number of colors N and fermionic flavors N_f is shown explicitly.

Keywords: Lattice QCD, Lattice perturbation theory, Overlap action.

PACS numbers: 11.15.-q, 11.15.Ha, 12.38.G.

I. INTRODUCTION

In recent years there has been great progress toward the implementation of chirality preserving regularizations of gauge theories coupled to fermions on the lattice. In the two most widely studied approaches, overlap fermions and domain wall fermions (for recent reviews, see [1,2]), numerical simulations are already producing promising results.

Alongside with numerical simulations, a number of perturbative calculations have also been carried out [3–6], which allow for a meaningful comparison between lattice results and continuum quantities. However, unlike the more conventional fermionic actions, the complexity of the overlap and domain wall actions has hampered the scope of perturbative results, and has kept the order of perturbative calculations down to 1 loop.

In this paper we perform a first 2-loop calculation using the overlap-Dirac fermionic action. The quantity we compute is the expectation value of the plaquette, in $SU(N)$ gauge theory coupled to N_f massless fermionic species. Aside from serving as a longtime testing ground for lattice perturbation theory, the plaquette operator has appeared in a variety of lattice investigations. One of its earliest uses has been in attempts to extract the quadratic gluonic condensate [7,8]. Another use regards the definition of an effective coupling constant [9,10], in an effort to improve the scaling properties of observables; this definition leads also to a modification of asymptotic scaling, which involves higher-loop coefficients of the plaquette. Finally, the plaquette is a standard ingredient in studies of the quark-antiquark potential (see, e.g., [11] and references therein).

In standard notation, we write the gluonic and fermionic parts of the action as follows:

$$S = S_G + S_F, \quad S_G = \beta \sum_{\square} E_G(\square), \quad S_F = \sum_{x,y} E_F(x,y) \quad (1)$$

with

$$\begin{aligned} \sum_{\square} E_G(\square) &= \sum_{\square} \left(1 - \frac{1}{N} \text{Re Tr}(\square) \right) \\ &= \frac{1}{2} \sum_x \sum_{\mu \neq \nu} \left(1 - \frac{1}{N} \text{Re Tr} (U_{x,x+\hat{\mu}} U_{x+\hat{\mu},x+\hat{\mu}+\hat{\nu}} U_{x+\hat{\mu}+\hat{\nu},x+\hat{\nu}} U_{x+\hat{\nu},x}) \right), \end{aligned} \quad (2)$$

$$E_F(x,y) = \sum_{i=1}^{N_f} a^4 \bar{\psi}_i(x) D_N(x,y) \psi_i(y) \quad (3)$$

As usual, $\beta \equiv 2N/g_0^2$ is the lattice coupling and a is the lattice spacing; \square stands for the plaquette and $U_{x,x+\hat{\mu}}$ for the link variable joining neighboring sites in the $\hat{\mu}$ direction: x and $x+\hat{\mu}$. The Neuberger-Dirac fermionic operator D_N depends on the link variables; its precise form will be presented below.

The average value of the action density, S/V , is directly related to the average plaquette; in particular, for the gluonic part we have:

$$\langle S_G/V \rangle = 6 \beta \langle E_G(\square) \rangle, \quad \langle E_G(\square) \rangle = 1 - \frac{1}{N} \langle \text{Tr}(\square) \rangle. \quad (4)$$

As for $\langle S_F/V \rangle$, it is trivial in any action which is bilinear in the fermion fields [10]; this can be seen by rescaling S_F in the fermionic partition function by a factor ϵ :

$$Z^F(\epsilon) \equiv \int [\mathcal{D}\bar{\psi}_i \mathcal{D}\psi_i] \exp(-\epsilon S_F) = \epsilon^{4VNN_f} Z^F(\epsilon = 1) \quad (5)$$

There follows:

$$\langle \sum_y E_F(x, y) \rangle = -\frac{\partial}{\partial \epsilon} \left(\frac{\ln Z^F(\epsilon)}{V} \right)_{\epsilon=1} = -4NN_f \quad (6)$$

We will thus calculate $\langle E_G(\square) \rangle$ in perturbation theory:

$$\langle E_G \rangle = c_1 g_0^2 + c_2 g_0^4 + c_3 g_0^6 + \dots \quad (7)$$

The n -loop coefficient can be written as $c_n = c_n^G + c_n^F$ where c_n^G is the contribution of diagrams without fermion loops and c_n^F comes from diagrams containing fermions. The coefficients c_n^G have been known for some time up to 3 loops [12,10]; more recently, some estimates for higher loops have been produced in 4 dimensions using stochastic methods [13], in the absence of fermions. The coefficients c_n^F are also known to 3 loops for Wilson fermions [10] and clover fermions [14]. The task at hand, c_n^F for overlap fermions, presents many more complications, and we will be computing c_2^F in the present work.

The calculation of c_n proceeds most conveniently by computing first the free energy $-(\ln Z)/V$, where Z is the full partition function

$$Z \equiv \int [DU \mathcal{D}\bar{\psi}_i \mathcal{D}\psi_i] \exp(-S). \quad (8)$$

The average of E_G is then extracted as follows

$$\langle E_G \rangle = -\frac{1}{6} \frac{\partial}{\partial \beta} \left(\frac{\ln Z}{V} \right). \quad (9)$$

In particular, the perturbative expansion of $(\ln Z)/V$:

$$(\ln Z)/V = \text{constant} + \left(-\frac{3(N^2 - 1)}{2} \ln \beta + \frac{d_1}{\beta} + \frac{d_2}{\beta^2} + \dots \right) \quad (10)$$

leads immediately to the relations: $c_2 = d_1/(24N^2)$, $c_3 = d_2/(24N^3)$.

A total of 8 Feynman diagrams contribute to the present calculation, up to 2-loop order; these are shown in Figure 1.

All the algebra necessary to carry out this calculation was done with our computer package written in Mathematica; to this end, certain extensions of the package were needed, in order to incorporate the numerical integration of 2-loop expressions involving overlap fermions. The first 6 diagrams in Figure 1 give the purely gluonic contributions to the free energy: c_1^G , c_2^G , which are well known (see, e.g., [10]). Their contribution is presented here for the sake of completeness:

$$\begin{aligned} c_1^G &= \frac{N^2 - 1}{8N}, \\ c_2^G &= (N^2 - 1) \left(0.0051069297 - \frac{1}{128N^2} \right) \end{aligned} \quad (11)$$

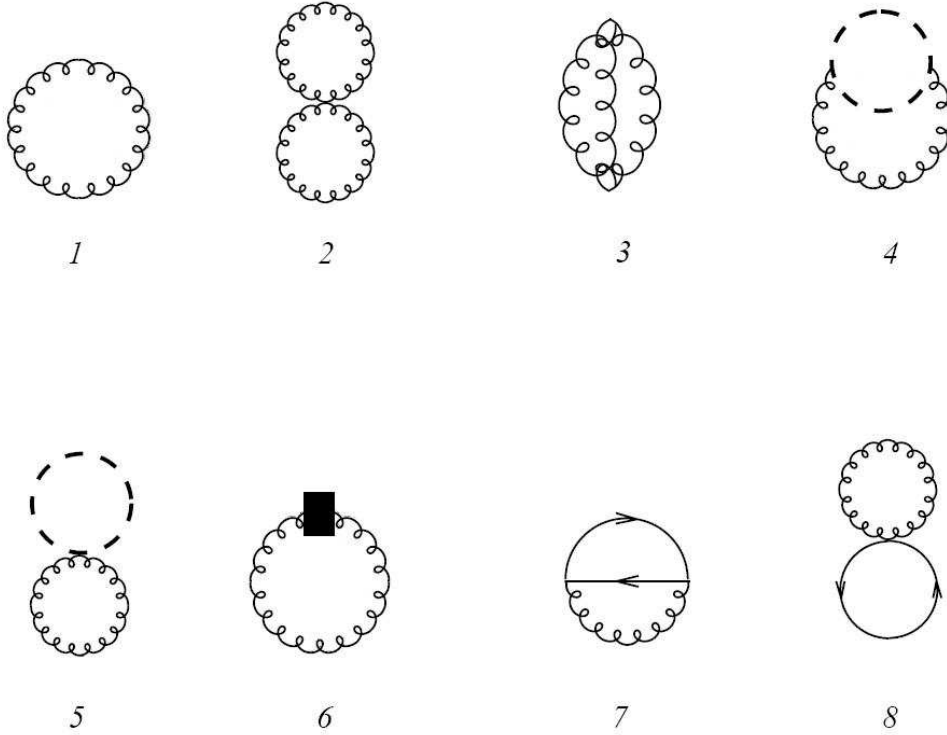


Fig. 1 Feynman diagrams contributing to the free energy up to 2 loops. Solid, wavy, dashed lines denote fermions, gluons and ghosts, respectively. A solid square stands for a contribution from the measure part of the action.

Diagrams 7 and 8 are much more cumbersome to calculate; they lead to the value of c_2^F , whose dependence on N and N_f can be made explicit:

$$c_2^F = \frac{N^2 - 1}{12 N} N_f h_2, \quad (12)$$

where h_2 is the quantity we set out to calculate; it depends only on a parameter M_0 which appears in the overlap action, to which we now turn.

The Neuberger-Dirac operator D_N appearing in the fermionic part of the action, Eq.(3), has the form [15]:

$$D_N = \frac{1}{a} M_0 \left(1 + X \frac{1}{\sqrt{X^\dagger X}} \right), \quad (13)$$

$$X = a D_W - M_0, \quad (14)$$

where D_W is the Wilson-Dirac operator (with the Wilson parameter r set to its standard value, $r = 1$)

$$D_W = \frac{1}{2} [\gamma_\mu (\nabla_\mu^* + \nabla_\mu) - a \nabla_\mu^* \nabla_\mu], \quad \nabla_\mu \psi(x) = \frac{1}{a} [U(x, \mu) \psi(x + a\hat{\mu}) - \psi(x)], \quad (15)$$

M_0 is a real parameter, whose value may be chosen at will; in order for this action to describe one massless fermion, with no doubling problem, M_0 must lie in the range $0 < M_0 < 2$. Nonperturbatively one expects $-m_c < M_0 < 2$, where $m_c < 0$ is the critical mass associated with the Wilson-Dirac operator.

Despite the non-ultralocal nature of the square root $[X^\dagger X]^{1/2}$, the operator D_N is nevertheless local under reasonable assumptions regarding the gauge configuration [16]. In particular, the expansion of D_N to all orders in perturbation theory, while very elaborate, poses no conceptual obstacle and can be performed starting from an integral representation of the square root [17].

The expressions for the overlap propagator and vertices are presented in the Appendix. It is worth noting that, by the nature of the overlap operator, the fermion vertex with two gluons contains two distinct parts: $\Sigma_2 = \Sigma_{2\alpha} + \Sigma_{2\beta}$ (see Appendix A); the first of these is pointlike, while the second involves integration over an internal four-momentum, as shown in Fig. 5. Consequently, diagram 8 splits into parts 8a, 8b; diagram 8b has the same topology as diagram 7.

The numerical integration over loop momenta was carried out for a wide range of values for $0 < M_0 < 2$ on finite lattices of size $L \leq 128$, with subsequent extrapolation to infinite size. The systematic error resulting from the extrapolation is typically small enough to leave the first six significant digits intact. A very slight reduction in precision is noticed as $M_0 \rightarrow 2$, where the pole structure of the fermionic propagator is expected to change.

Our results, as a function of M_0 , are presented in Figure 2 for each fermionic diagram separately; their sum is shown in Figure 3 and listed in Table I. It is worth noting that the results are very smooth functions of M_0 , despite the potential singularities of the integrands at $M_0 = 0$ and $M_0 = 2$.

To facilitate comparison, we provide below the values of individual diagrams for a particular value of M_0 :

$$\begin{aligned} h_2^7(M_0=1) &= -0.02013079(1), & h_2^{8\alpha}(M_0=1) &= -0.0099775548(1), \\ h_2^{8\beta}(M_0=1) &= 0.010764939(1) \end{aligned} \quad (16)$$

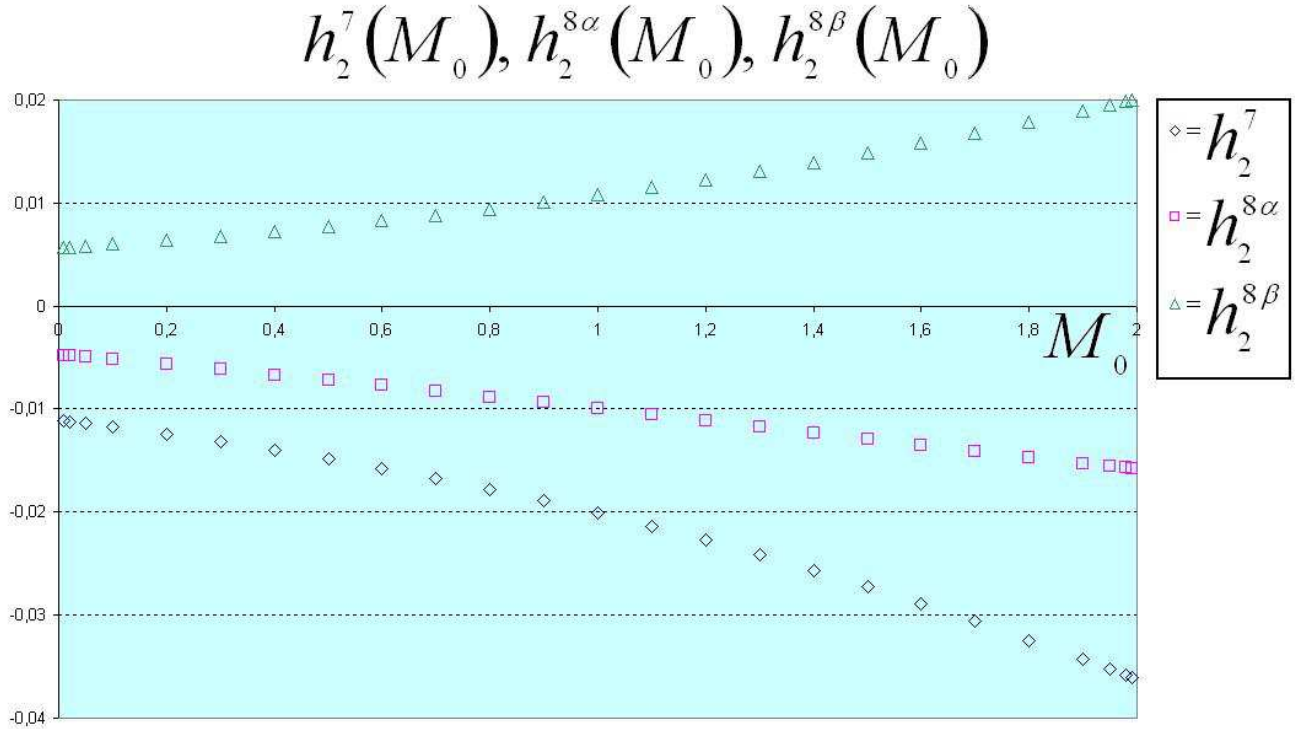


Fig. 2 Numerical results for each diagram involving fermions, as a function of the parameter M_0 . The values denoted by 8α and 8β correspond to the two contributions to diagram 8, coming from vertices $\Sigma_{2\alpha}$ and $\Sigma_{2\beta}$, respectively.

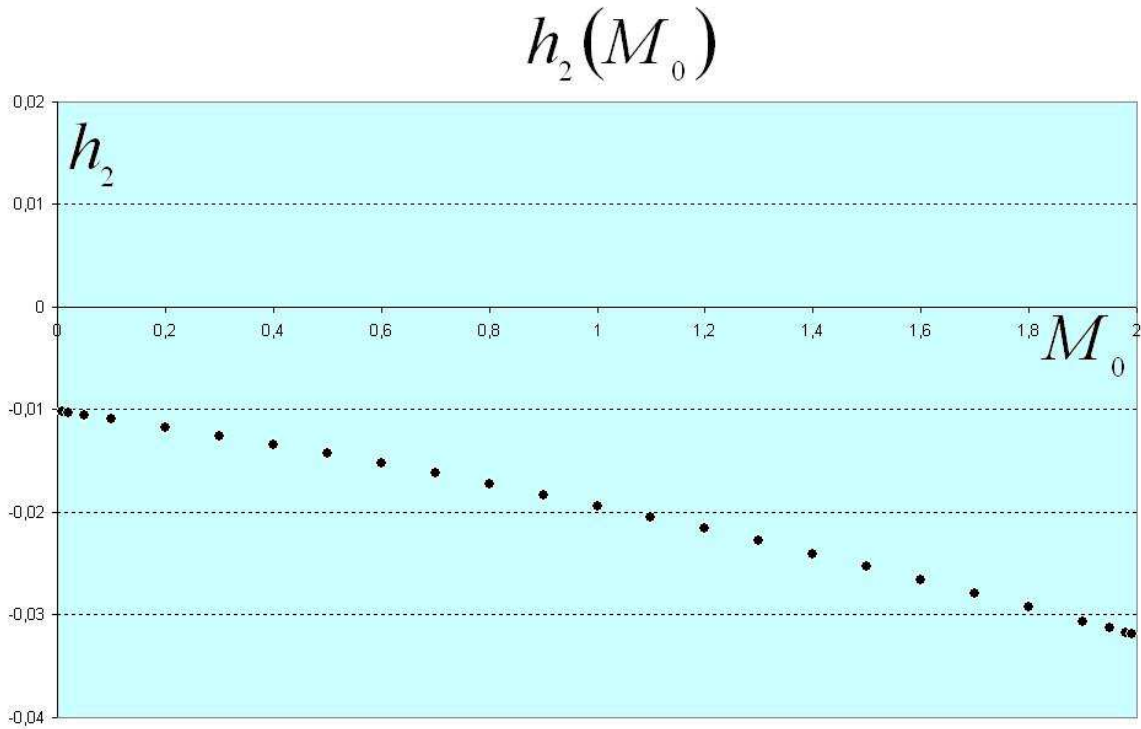


Fig. 3 The total contribution of fermionic diagrams to h_2 , as a function of the parameter M_0 .

For ease of reference, we list below the total value of $\langle E_G(\square) \rangle$ for $N = 3$ and $N_f = 0, 2, 3$, with some typical values of the action parameters (κ is the hopping parameter of the Wilson action):

$$\begin{aligned}
\langle E_G(\square) \rangle &= g_0^2/3 + g_0^4 \cdot 0.033910993 && (N_f = 0) \\
&= g_0^2/3 + g_0^4 \cdot 0.0234689 && (N_f = 2 \text{ Wilson, } r = 1, \kappa = 0.156) \\
&= g_0^2/3 + g_0^4 \cdot 0.0253139 && (N_f = 2 \text{ overlap, } M_0 = 1.0) \\
&= g_0^2/3 + g_0^4 \cdot 0.0226752 && (N_f = 2 \text{ overlap, } M_0 = 1.5) \\
&= g_0^2/3 + g_0^4 \cdot 0.0182479 && (N_f = 3 \text{ Wilson, } r = 1, \kappa = 0.156) \\
&= g_0^2/3 + g_0^4 \cdot 0.0210154 && (N_f = 3 \text{ overlap, } M_0 = 1.0) \\
&= g_0^2/3 + g_0^4 \cdot 0.0170573 && (N_f = 3 \text{ overlap, } M_0 = 1.5)
\end{aligned} \tag{17}$$

The extension of the above calculation in order to encompass Wilson loops of larger size, as may be required for computing the quark-antiquark potential, presents no additional difficulties. Further two-loop calculations with the overlap action involve fermionic vertices with 3 and 4 gluons; generating these vertices is conceptually straightforward, though technically it is quite involved. We are presently working on these extensions, and expect to provide results in a future report.

APPENDIX A

We present here the expressions for the overlap propagator and for the fermionic vertices containing up to two gluons, following Refs. [17,3]. This Appendix serves for completeness, and also in order to correct some typographical errors (which had no consequence on previous results).

Let us first write down the weak coupling expansion of the Wilson-Dirac operator D_W . This will be useful for constructing the relevant vertices of D_N . We write

$$\begin{aligned}
X(q, p) &\equiv a^4 \sum_{x,y} e^{-iq \cdot x + ip \cdot y} (D_W(x, y) - \frac{M_0}{a} \delta_{x,y}) \\
&= X_0(p)(2\pi)^4 \delta^4(q - p) + X_1(q, p) + X_2(q, p) + \mathcal{O}(g_0^3),
\end{aligned} \tag{A1}$$

$$\text{where : } \quad X_0(p) = \frac{i}{a} \sum_{\mu} \gamma_{\mu} \sin ap_{\mu} + \frac{1}{a} \sum_{\mu} (1 - \cos ap_{\mu}) - \frac{1}{a} M_0, \tag{A2}$$

$$X_1(q, p) = g_0 \int d^4 k \delta(q - p - k) A_{\mu}(k) V_{1,\mu}(p + k/2), \tag{A3}$$

$$V_{1,\mu}(q) = i\gamma_{\mu} \cos aq_{\mu} + \sin aq_{\mu},$$

$$X_2(q, p) = \frac{g_0^2}{2} \int \frac{d^4 k_1 d^4 k_2}{(2\pi)^4} \delta(q - p - k_1 - k_2) A_{\mu}(k_1) A_{\mu}(k_2) V_{2,\mu}(p + k_1/2 + k_2/2), \tag{A4}$$

$$V_{2,\mu}(q) = -i\gamma_{\mu} a \sin aq_{\mu} + a \cos aq_{\mu}.$$

The Fourier transform of the Neuberger-Dirac operator takes the form

$$\frac{1}{M_0}D_N(q, p) = D_0(p)(2\pi)^4\delta^4(q - p) + \Sigma(q, p). \quad (\text{A5})$$

The factor $1/M_0$ in the above equation is inconsequential, since it can be absorbed in the definition of $\psi(x)$. $D_0(p)$ is the tree level inverse propagator:

$$D_0^{-1}(p) = \frac{-i \sum_{\mu} \gamma_{\mu} \sin ap_{\mu}}{2 [\omega(p) + b(p)]} + \frac{a}{2}, \quad (\text{A6})$$

$$\text{where : } \quad \omega(p) = \frac{1}{a} \left(\sum_{\mu} \sin^2 ap_{\mu} + \left[\sum_{\mu} (1 - \cos ap_{\mu}) - M_0 \right]^2 \right)^{1/2}, \quad (\text{A7})$$

$$b(p) = \frac{1}{a} \sum_{\mu} (1 - \cos ap_{\mu}) - \frac{1}{a} M_0. \quad (\text{A8})$$

The function $\Sigma(q, p)$ can be expanded in powers of g_0 as

$$\begin{aligned} a\Sigma(q, p) = & \frac{1}{\omega(q) + \omega(p)} \left[X_1(q, p) - \frac{1}{\omega(q)\omega(p)} X_0(q) X_1^{\dagger}(q, p) X_0(p) \right] \\ & + \frac{1}{\omega(q) + \omega(p)} \left[X_2(q, p) - \frac{1}{\omega(q)\omega(p)} X_0(q) X_2^{\dagger}(q, p) X_0(p) \right] \\ & + \int \frac{d^4k}{(2\pi)^4} \frac{1}{\omega(q) + \omega(p)} \frac{1}{\omega(q) + \omega(k)} \frac{1}{\omega(k) + \omega(p)} \times \\ & \left[-X_0(q) X_1^{\dagger}(q, k) X_1(k, p) - X_1(q, k) X_0^{\dagger}(k) X_1(k, p) - X_1(q, k) X_1^{\dagger}(k, p) X_0(p) \right. \\ & \left. + \frac{\omega(q) + \omega(k) + \omega(p)}{\omega(q)\omega(k)\omega(p)} X_0(q) X_1^{\dagger}(q, k) X_0(k) X_1^{\dagger}(k, p) X_0(p) \right] + \mathcal{O}(g_0^3) \quad (\text{A9}) \end{aligned}$$

From $\Sigma(q, p)$ one can read off the vertices containing up to two gluons. The vertex with one gluon, $a\Sigma_1(q, p)$ corresponds to the first line of Eq.(A9).



Fig. 4 Pointlike part of the vertex.

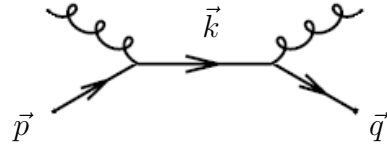


Fig. 5 Vertex part with intermediate momentum integration

The fermionic vertex with two gluons splits into a pointlike part $a\Sigma_{2\alpha}$ (Fig. 4, second line of Eq.(A9)) plus a part involving an internal four-momentum k , which must be integrated over, $a\Sigma_{2\beta}$ (Fig. 5, last 3 lines of Eq.(A9)).

TABLE I. Two-loop fermionic contribution h_2 , for various values of M_0 , $0 < M_0 < 2$.

M_0	h_2
0.01	-0.01021118(5)
0.05	-0.01050736(5)
0.1	-0.01088833(5)
0.2	-0.01168252(5)
0.4	-0.01338658(3)
0.6	-0.01523365(1)
0.8	-0.01721907(1)
1.	-0.01934341(1)
1.2	-0.02160970(1)
1.4	-0.02402085(3)
1.6	-0.02657516(3)
1.8	-0.02925538(3)
1.9	-0.03062501(5)
1.95	-0.03130974(5)
1.99	-0.0318533(3)

REFERENCES

- [1] T. Chiu, Nucl. Phys. B (PS) **129-130C** (2004) 135.
- [2] S. Chandrasekharan, U.-J. Wiese, Prog. Part. Nucl. Phys. **53**, issue 1 (2004).
- [3] C. Alexandrou, H. Panagopoulos, E. Vicari, Nucl. Phys. **B571** (2000) 257; C. Alexandrou, E. Follana, H. Panagopoulos, E. Vicari, Nucl. Phys. **B580** (2000) 394.
- [4] S. Capitani, Nucl. Phys. **B597** (2001) 313; **B592** (2001) 183; S. Capitani, L. Giusti, Phys. Rev. **D62** (2000) 114506.
- [5] R. Horsley et al., Nucl. Phys. **B693** (2004) 3.
- [6] N. Yamada, S. Aoki, Y. Kuramashi, arXiv:hep-lat/0407031.
- [7] A. Di Giacomo, G. C. Rossi, Phys. Lett. **B100** (1981) 481.
- [8] B. Allés et al., Phys. Rev. **D48** (1993) 2284.
- [9] G. Martinelli, G. Parisi, R. Petronzio, Phys. Lett. **B100** (1981) 485.
- [10] B. Allés, A. Feo, H. Panagopoulos, Phys. Lett. **B426** (1998) 361.
- [11] B. Bali, P. Boyle, “Perturbative Wilson loops with massive sea quarks on the lattice”, arXiv:hep-lat/0210033.
- [12] B. Allés, M. Campostrini, A. Feo, H. Panagopoulos, Phys. Lett. **B324** (1994) 433.
- [13] F. Di Renzo, L. Scorzato, JHEP **0110** (2001) 038.
- [14] H. Panagopoulos, A. Tsapalis, Univ. of Cyprus preprint UCY-23/04; A. Athenodorou, H. Panagopoulos, A. Tsapalis, Proceedings, Lattice 2004; A. Athenodorou, Bachelor’s Thesis, Univ. of Cyprus (2004, in Greek); M. Ioannou, Bachelor’s Thesis, Univ. of Cyprus (2004, in Greek).

- [15] H. Neuberger, Phys. Lett. **B417** (1998) 141; **B427** (1998) 353.
- [16] P. Hernández, K. Jansen, M. Lüscher, Nucl. Phys. **B552** (1999) 363.
- [17] Y. Kikukawa, A. Yamada, Phys. Lett. **B 448** (1999) 265.